EUROPEAN MICROWAVE ASSOCIATION — EuMA

Prototype design of a dual-band dual-polarization Ku/Ka-band feed

Hendrik A. Thiart[1], K. Rambabu[2] and Jens Bornemann[3]

Abstract – A design approach for a Ku/Ka-band satellite antenna feed prototype is presented. Band separation is achieved by employing a dielectrically loaded circular waveguide. To allow cost-effective integration with other components, etched probes formed from the same substrate board as surrounding circuitry are introduced as Ku-band coupling structures in the dual-band waveguide cavity. Design and fabrication of the prototype feed are discussed. Predicted and measured results are presented to support proof of concept.

Index Terms – Dielectric loaded antennas, Dielectric loaded waveguides, Reflector antenna feeds, Multiplexing, Polarization, Waveguide junctions, Waveguide transitions, Microstrip circuits.

I. Introduction

Satellite based communication systems lend themselves well to the expansion of broadband applications to commercial and consumer markets due to the logistical and frequency use advantages over cable based technologies. Specifically in Europe, where television reception systems already exists in the absence of a prolific cable network, the opportunity arose to use the existing DBS (direct broadcast by satellite) infrastructure with the addition of an RCS (return channel system) component. The satellite dish antenna system deployed at the user site requires low cost and relatively small size solutions that in turn dictate a significant degree of system integration and ease of manufacturing. This paper introduces a possible solution for the associated feed component that enables such integration with the associated LNB (low-noise block). Note that system aspects such as specific dish-feed integration and trade-offs between feed loss and specific LNB gain and noise figure are not considered for this prototype. Moreover, the development of this component proceeded under a compromise between performance and low-cost fabrication. Further development will be necessary to address some of the issues raised in Section IV.

Fig. 1 shows a transparent view of the feed. In order to effectively handle the Ku-band (10.7 GHz -12.75 GHz) and Ka-band (29.5 GHz - 30 GHz) signals within the same waveguide structure, a circular waveguide loaded by a dielectric rod is used in [1] and subsequently investigated by others [2] - [5]. The Ka-band is used for transmission and is launched into the feed through a WR28 waveguide plate that can be rotated by 90^0 in order to set the desired linear polarization orientation for the Ka-band. The signal passes through a dielectrically filled circular waveguide section that ends in the larger Ku-band circular waveguide cavity. The dielectric extends from this point forward as a dielectric rod that largely contains the Ka-band signal within an HE_{11} mode until it is radiated from the rod at the aperture of the horn.

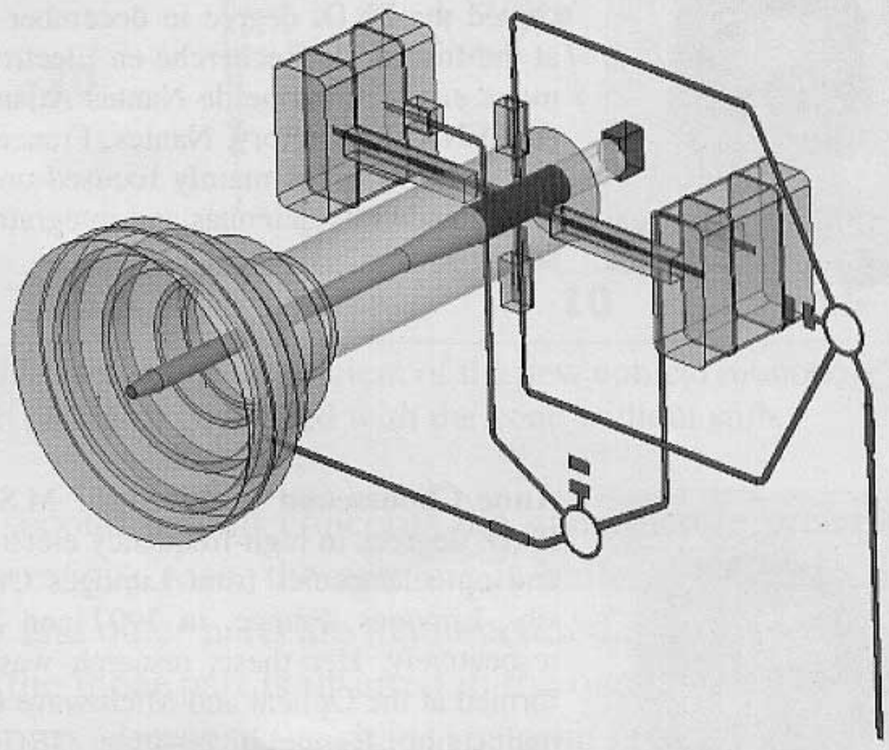

Fig. 1. Transparent view of the dual-band dual-polarization prototype feed.

The Ku-band signal (used for reception) enters the feed by means of a coaxially corrugated horn and propagates through the structure as a quasi-TE_{11} mode in the dielectric rod loaded circular waveguide. Towards the back of the structure, a coaxial waveguide section is used to separate four substrate probes from the HE_{11} Ka-band mode. The probes are etched from the substrate board that will be used to carry the associated LNB circuitry and are used to couple the incoming Ku-band signal from the feed. Both vertical and horizontal linear polarization availabilities are required, and each pair of opposite probes is used to couple out one of the incoming Ku-band polarizations. Since the quasi-TE_{11}-mode field distribution excites the two corresponding balanced probes with current distributions that are 180^0 out of phase, the signals from the two probes are combined by 180^0hybrid rat-race couplers, as reported in, e.g., [6] and [7].

Note that in contrast to components presented in [4] and [5], our design avoids the machining of an actual coax-

Received May 17th, 2006. Revised October 6th, 2006.

[1] Adventenna Inc., 4800 Patrick Henry Drive, Santa Clara, Ca 95054, USA; [2] Institute for Infocomm Research, 02-21/25 TeleTech Park, 20 Science Park Road, Singapore Science Park II, Singapore 117674; [3] Department of Electrical and Computer Engineering, University of Victoria, Victoria, BC, Canada V8W 3P6.

ial waveguide section. Our coaxial section is created by wrapping copper foil around the dielectric rod and soldering it to a copper protrusion at the back of the feed. This reduces fabrication complexity and costs. Moreover, and associated with the avoidance of a machined coaxial section, the band-reject filters presented in [4] as waveguide irises and in [5] as coaxial irises are omitted here in order to investigate whether a functional response can be obtained for both bands without the separation of the Ka-band from the Ku-band multiplexer structures in the main feed-multiplexer cavity.

In order to avoid the crossing of the related microstrip lines leading to the two rat-race combiners, the second combiner was moved to a second circuit board and the required signals coupled through rectangular waveguide coupling sections. It should be noted that these structures could be replaced by other methods of crossing the related Ku-band polarization signals. For instance, a three-layer board, with the probe pairs etched on opposite sides of the center ground plane laminate, would be an option. For the specific budgetary and low-cost manufacturing constraints, the coupling passages presented the safest return of a functional prototype to investigate the actual measured operation of the feed against the predicted and simulated design responses. Finally, matching sections are added in the microstrip circuitry to improve the return loss of the two Ku-band output ports.

II. Design

The dielectric rod within the feed is designed as a stand-alone rod antenna as described in [8]. In order to determine the dimensional parameters, the propagation constant of the HE_{11} mode and the cutoff frequencies of the next higher-order modes in the dielectric rod are calculated according to [9]. It is found that the diameter of the rod in the main propagation section of the feed can be chosen based on the mono-modal operation criteria given in [8]. (Note that we refrain from presenting this entire investigation for lack of space. The interested reader is referred to [10] for details.)

A further concern is breakdown of the assumed HE_{11} hybrid mode when the diameter of the dielectric rod becomes too low for proper mode containment at the lowest frequency of operation, given a certain dielectric constant. The latter sets a lower limit to the rod diameter and the former criteria sets an upper limit. A value is chosen for the diameter such that manufacturing tolerances would not cause the diameter to go below the lower limit. The propagation constant of the HE_{11} mode in the dielectric rod of chosen diameter is used to design the dimensions of the dielectric rod radiator following [8]. The lengths and diameters of the two rod tapers from this initial design are kept constant for the rest of the design. Only the length of the rod is optimized in a later design stage. In order for the coaxial waveguide section to function properly, the dielectric-filled circular waveguide section needs to be in cut off for the Ku-band. Once the initial design of the dielectric rod is completed, this cut off is verified before proceeding with the design.

Next the outer radius of the main propagation section circular waveguide is designed such that mono-modal quasi-TE_{11} operation for the Ku-band is assured. Note that the presence of the dielectric rod causes the field distribution of the pure TE_{11} mode to vary slightly. This difference is negligible, however, as long as the dielectric constant of the dielectric rod is low enough and the diameter of the rod small enough [11]. For a dielectric constant of 2.55 and the rod diameter resulting from the dielectric rod design, these criteria are met. To determine the modal cut off frequencies of the circular waveguide loaded by a dielectric rod, a similar approach as that for the dielectric rod design is taken. The dielectric rod diameter is kept fixed and the outer circular waveguide dimension varied. This approach allows for a proper choice of the outer circular waveguide radius.

The coaxially corrugated Ku-band waveguide horn was chosen for its good radiation characteristics combined with the ease of manufacturing as opposed to a regular corrugated horn. This component was taken from an existing design courtesy of Norsat Intl. Inc.

The remainder of the design was completed by a parametric study approach using the Finite-Element Method full-wave solver HFSS and Agilent ADS. The etched probe design (c.f. Fig. 1) is first modeled as probes coupling into an empty coaxial circular waveguide in order to determine initial values for the probe length and backshort-wall distance, similar to the study performed in [12], [13] for rectangular waveguide fed by etched probes. Subsequently, the full structure of the feed including the dielectric rod and Ku-band horn is introduced, and the probe length, backshort-wall distance and length of the coaxial waveguide center structure are optimized for proper S-parameter and radiation pattern performance.

Since the Ka-band propagation is a combination of the HE_{11} mode, launched into the dielectric rod at the end of the coaxial waveguide center structure, and a radiated wave excited at the same junction [8], the Ka-band energy is not completely contained in the dielectric rod. The final Ka-band radiating aperture field distribution is a combination of the HE_{11}-mode radiation from the end of the rod and the radiated wave excited at the coaxial center structure edge, propagating to the horn aperture. Consequently, the Ku-band structures of the coaxial waveguide interact with the backward traveling radiated Ka-band wave and influence the Ka-band return loss and radiation response. The dimensions of the feed structures must therefore be optimized to achieve a proper dual-band response. The length of the coaxial waveguide section center structure, length of the total feed including the Ku-band horn, length of the dielectric rod and length of the dielectric-filled circular waveguide that extends from the back of the feed to the WR28 waveguide, are used in a parametric study opti-

mization to achieve this goal.
The rectangular waveguide coupling passages in Fig. 1 for passing one of the Ku-band polarizations to the second microstrip board are also analyzed and optimized in a parametric study using HFSS.
Once the dimensions of the feed and waveguide coupling passages are finalized, the Ku-band S-parameters of the feed, as seen into the etched probes, are imported into an equivalent circuit analysis tool (Agilent ADS). Finally, the sections in microstrip technology are optimized for good return loss performance. These parameters include lengths and impedances of the matching sections between (i) the probes and the waveguide coupling passages, (ii) the probes and the rat-race combiners, e.g. [14], and (iii) the rat-race combiners and the Ku-band output ports (c.f. Fig. 1).

III. Prototype fabrication

As mentioned before, the Ku-band waveguide horn was taken from an existing component courtesy of Norsat Intl. Inc. The dielectric rod was turned out of a suitable dielectric material with ε_r=2.55. The use of etched probes on the same substrate board as surrounding circuitry necessitated the use of a sandwich structure for the metal housing. Three sections were manufactured. Fig. 2 and Fig. 3 show a center base plate for carrying the circuitry and a front and back plate to form the lids of the housing. The back plate also serves as mechanical support for the dielectric rod.

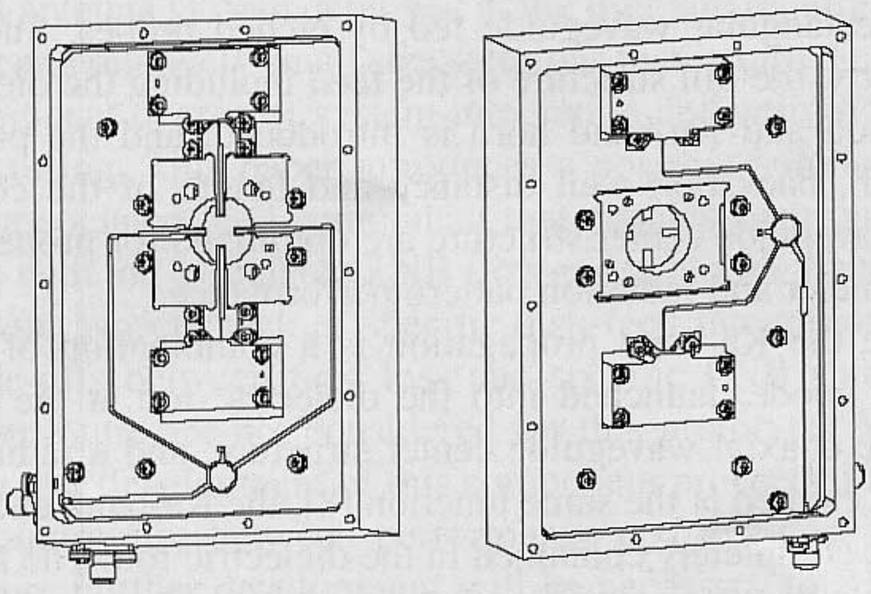

Fig. 2. Front view (left) and back view (right) of the housing base plate with the two attached substrate boards.

The wall thickness of the circular waveguide that encloses the back of the dielectric rod and forms the coaxial waveguide section center structure, needs to be as thin as possible to minimize the discontinuity presented to the Ku-band signal. Therefore, copper foil was wrapped around the rod and soldered to a copper protrusion on the back plate (Fig. 3) that also forms the backshort wall of the feed's coaxial waveguide section. Ohmic continuity for the circular waveguide is maintained by a protrusion of the front plate extending through a cut out of the substrate board to connect to the base plate. Similarly, the protrusion

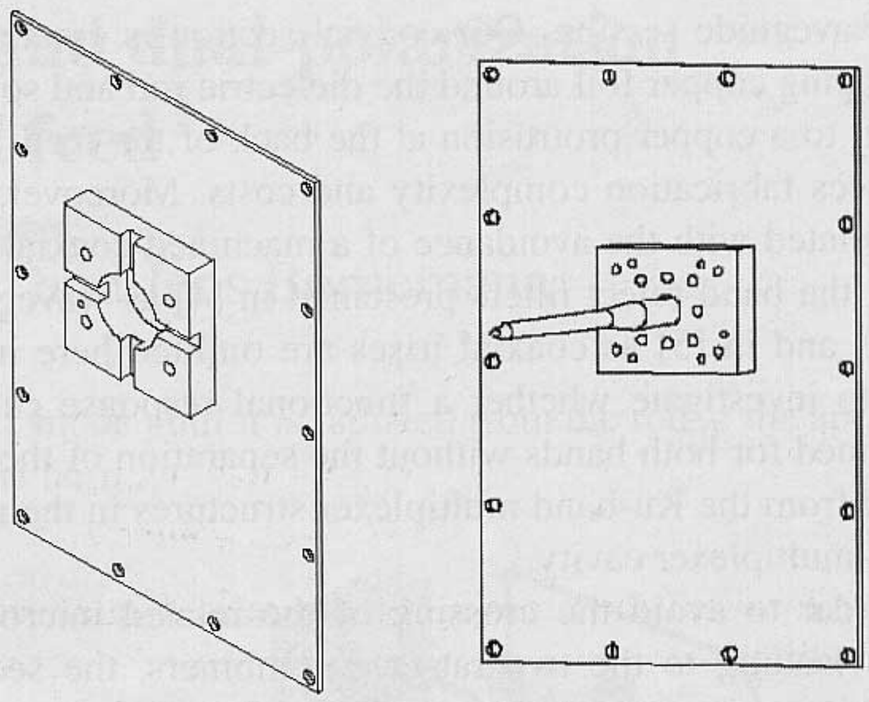

Fig. 3. Front plate (left) and back plate (right) of housing.

on the back plate extends through a cut out of the second substrate board to attach to the base plate.
A WR28 rotation plate is attached to the back of the housing via a symmetric screw hole pattern to be able to launch the Ka-band signal in two orthogonal polarizations. Coaxial SMA-type connectors were used as external connectors for the two Ku-band ports. Fig. 4 shows the assembled prototype used in obtaining the measured results.

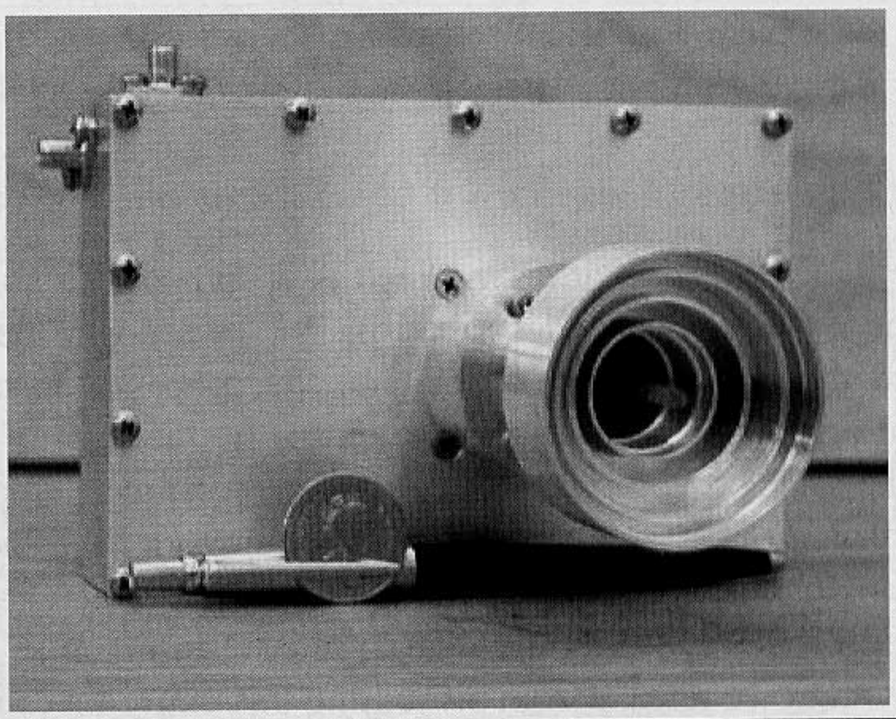

Fig. 4. Front view of the completed feed multiplexer and size comparison with a Canadian quarter coin.

IV. Results

A) Return Loss and Isolation

Fig. 5 shows the measured and simulated return loss response measured at the vertical and horizontal polarization ports of the prototype feed. In order to measure Ku-band connection to following amplifier circuitry, the effect of the SMA coaxial connectors was de-embedded by simulating the microstrip-to-coaxial connector transition in HFSS. Relatively good agreement between the measured and simulated response was achieved. Deviation from exact agreement can be attributed to the fact that the entire feed could not be simulated in HFSS. This necessitated a two-stage simulation with the S-parameter results from

HFSS imported as a data element in the equivalent circuit model ADS software and vice versa. Therefore, the simulated response for the feed in HFSS was used as an ideal case response neglecting the effects of the loading caused by the rest of the circuitry. The response of the actual measured component, however, includes the loading. Furthermore, the effects of the full feed's housing cavity on the microstrip circuitry could not be simulated and may have contributed to a change in response. However, for the purpose of designing for a certain maximum threshold to the response, the agreement is sufficient. The horizontal polarization shows a very good response across almost the entire band of operation. The vertical polarization response is worse towards the high end of the band. Possible reasons for the poorer response in the vertical polarization are slight deviations in manufacturing as well as possible poorer agreement of the actual soldered coaxial connector transition with the model used for de-embedding. Moreover, the ADS response in Fig. 5b should be viewed as shifted in frequency rather than disagreements per frequency point. Such a shift is common as ADS is not a full-wave analysis tool. These shortcomings, as well as the poor return loss towards the upper band limit, will have to be addressed in a future design stage.

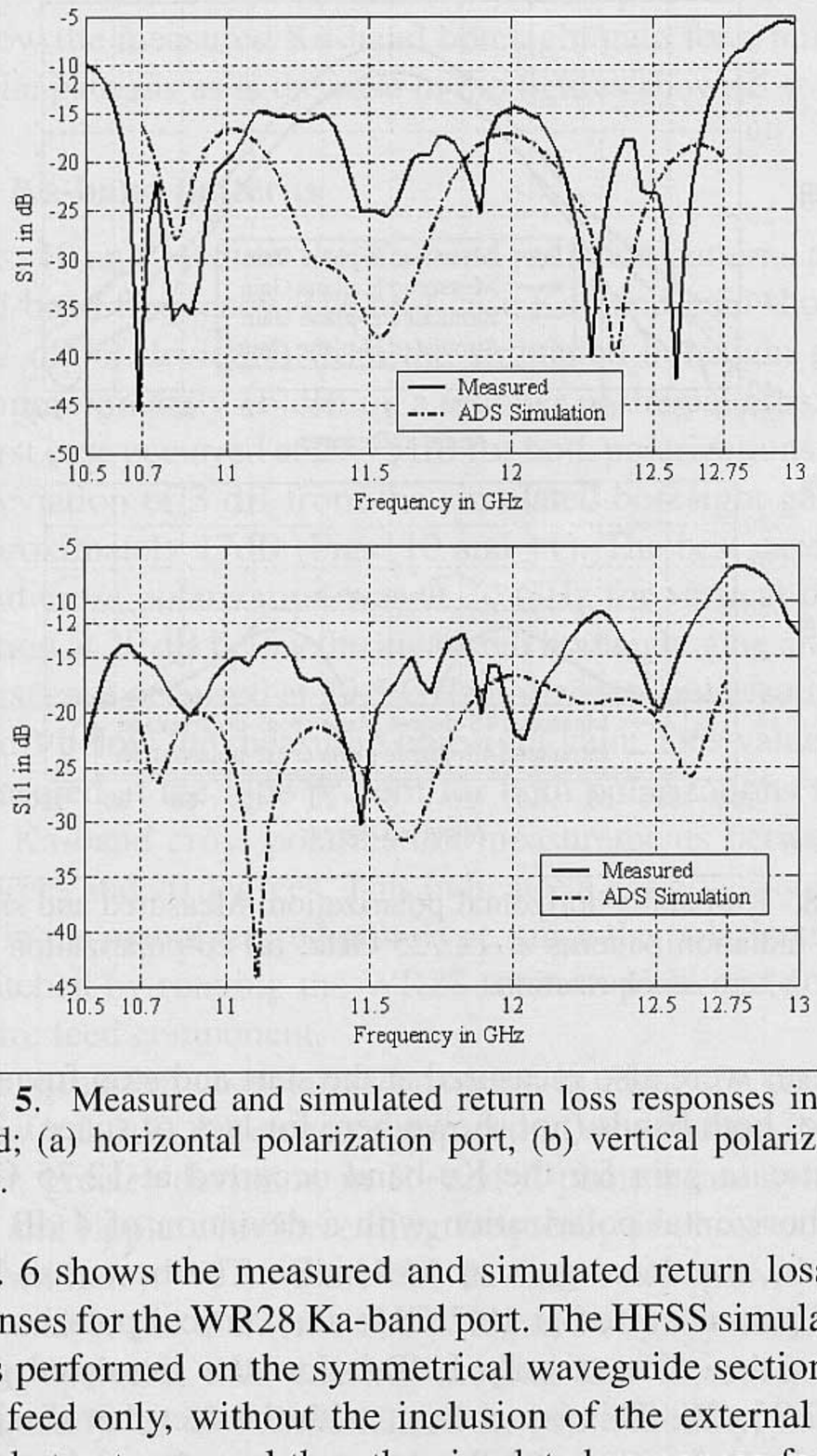

Fig. 5. Measured and simulated return loss responses in Ku-band; (a) horizontal polarization port, (b) vertical polarization port.

Fig. 6 shows the measured and simulated return loss responses for the WR28 Ka-band port. The HFSS simulation was performed on the symmetrical waveguide sections of the feed only, without the inclusion of the external Ku-band structures, and thus the simulated responses for the two polarizations are the same and represented by a single graph. The measured results, which include the entire feed structure, show that the loading of the external Ku-band structures did not affect the return loss of the two Ka-band polarizations differently. Therefore, an acceptable return loss for both polarizations is achieved. The length of the coaxial waveguide section affects the Ka-band return loss response and was confirmed by measurement to be as designed and simulated. The exact length and variations on the dielectric rod taper was more difficult to measure, however, and a slight deviation in the starting position and dimensions of the taper may have contributed to the deviation between the simulated and measured responses. Although further development-for-manufacturing work is likely to improve the performance, a functional Ka-band prototype is realized.

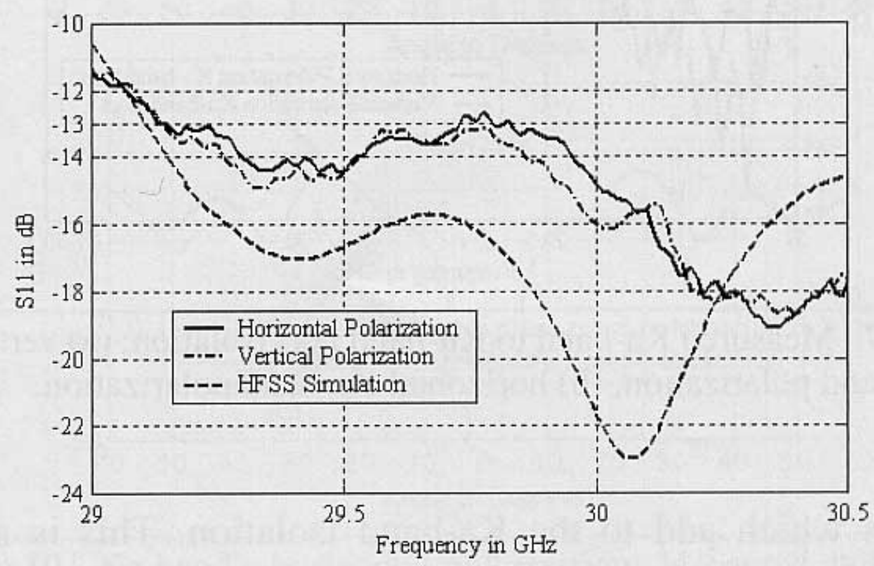

Fig. 6. Measured and simulated return loss responses in Ka-band.

Fig. 7 shows the measured isolation between the Ka-band input port and the respective Ku-band ports. This isolation is important since transmitted Ka-band power may detrimentally affect the amplifier and mixer stages in the Ku-band's LNB's if too much power leaks into the Ku-band circuitry.

The measurements were performed by removing the WR28 waveguide-to-coaxial connector transition from one of the two VNA test cables and connecting the remaining coaxial connector to the SMA connector of the applicable Ku-band port. As such, the previously used Ka-band LRL calibration had to be disturbed. Furthermore, the isolative effect of the Ku-band SMA connector at Ka-band is included in the measurement. As a result the measurements are not absolutely accurate and can only serve as an indication of the isolation. The worst response is the isolation between the vertically launched Ka-band and vertical polarization Ku-band port. This is to be expected since the co-polarized Ka-band signal in the feed will couple most strongly to the co-aligned probes of the vertical polarization Ku-band circuitry; i.e., a portion of the Ka-band radiated wave launched at the coaxial section end (mentioned in section II) travels back towards and couples to the vertical probes.

The co-polarization isolation in the horizontal case (Fig. 7b) is better by about 15 dB due to the fact that the Ku-band structure includes the waveguide coupling pas-

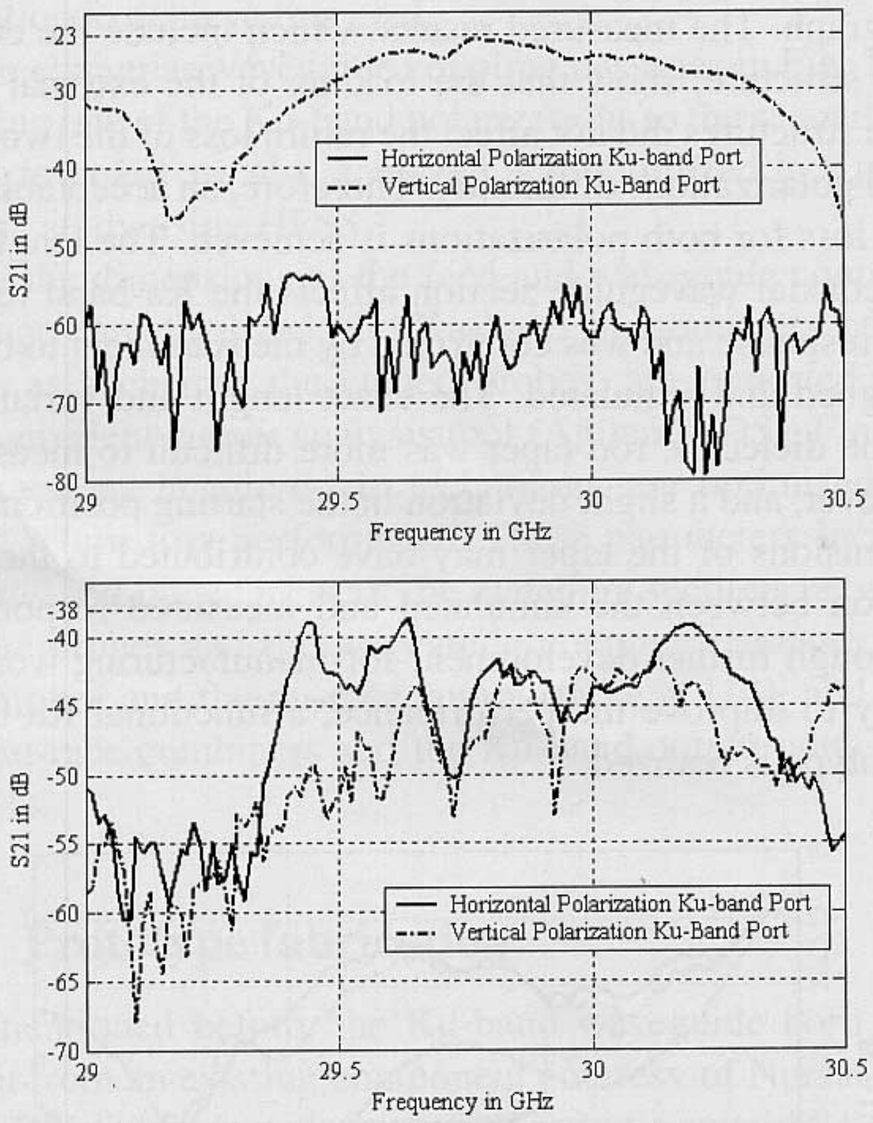

Fig. 7. Measured Ka-band to Ku-band port isolation; (a) vertical Ka-band polarization, (b) horizontal Ka-band polarization.

sages which add to the Ka-band isolation. This is also evident in the fact that the cross-polarized isolation of the vertically launched Ka-band and horizontal Ku-band port (Fig. 7a) is much better than that of the horizontally launched Ka-band and vertical Ku-band port (Fig. 7b) since the former includes the coupling passages in the Ku-band structures. Improved isolation requirements will necessitate the use of a filter to provide an additional attenuation of 15-20 dB, when operated with a transmitter power output of 2W. Contrary to positioning this filter within the waveguide as in [4] and [5], which considerably adds to manufacturing costs, it is recommended that such a filter be added to the vertical-polarization microstrip circuitry. The added losses of this filter need to be traded off with the LNB performance.

B) Ku-band patterns

Fig. 8 to Fig. 11 show the radiation pattern results at the center frequencies for the Ku- and Ka-bands (11.725 GHz and 29.5 GHz). Simulated radiation patterns were obtained from HFSS. The prototype radiation patterns were measured in a compact range at the University of Manitoba, Canada. The gain patterns are shown in dB relative to the listed absolute gain, which is the maximum (boresight) gain of the simulated patterns. Cross polarization patterns are shown in dB relative to the respective associated gain maxima; i.e., in Fig. 8, the measured cross polarization is approximately 25 dB below the measured gain maximum that in turn is 3 dB below the listed absolute gain of the simulated pattern.

Good agreements between the simulated and measured patterns are obtained in both bands. The Ku-band patterns show an approximate 3 dB difference between the simulated and measured maximum boresight gains. The reflective loss effects of the coaxial connectors that were de-embedded to obtain the feed measured return loss are included in the radiation pattern measurements. In adition the simulated gains do not include the full microstrip structure. In order to obtain an estimate of the losses incurred due to the microstrip circuitry, an analysis was performed in ADS and the reflective component due to return loss separated from the response. The results indicated that the microstrip circuitry introduced a loss of approximately 1dB. Depending on the reflector used and the noise associated with the active circuitry employed with the feed, a loss of 1 dB may be excessive. It should be noted, however, that the prototype circuit layout was carried out with an emphasis on ease of prototype manufacturing. For a commercial product, the circuit layout leading up to the first LNA stage of the LNB can be significantly shortened to improve the dissipative loss performance and reduce occupied board area. Ku-band cross polarization are acceptable at better than 25 dB in Fig. 8 and Fig. 9.

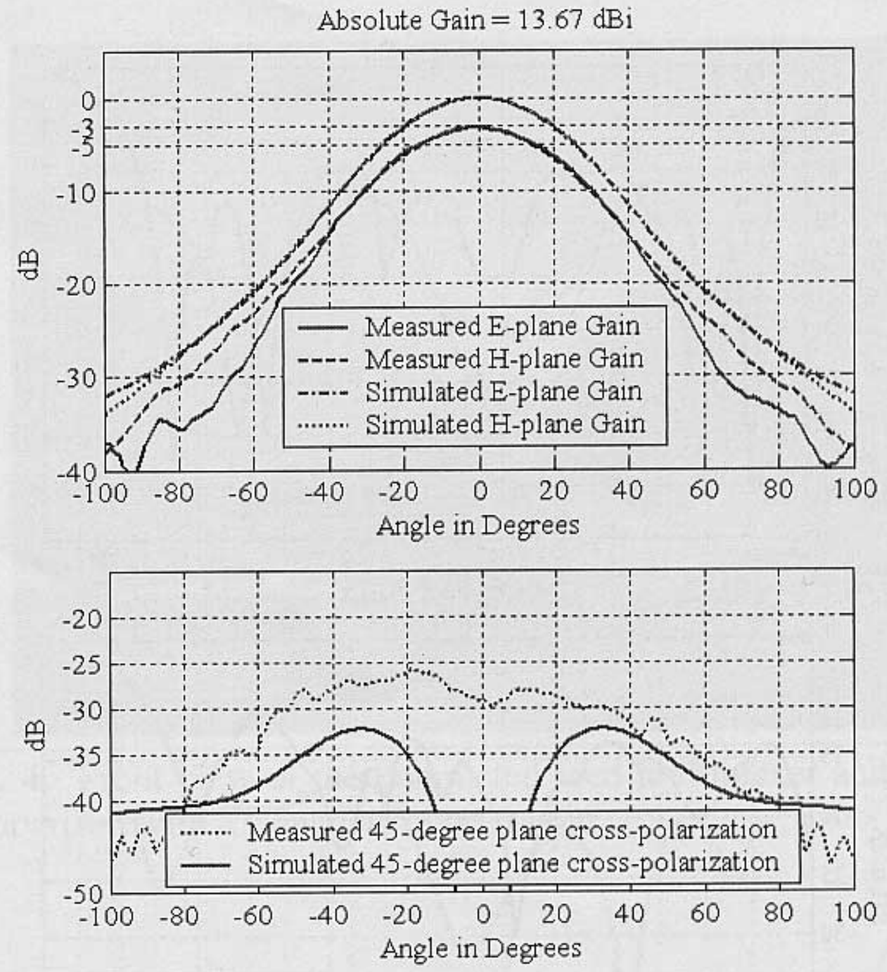

Fig. 8. Ku-band's horizontal polarization: Measured and simulated radiation patterns at 11.725 GHz; (a) co-polarization and gain, (b) cross polarization.

Patterns were also measured at the start and stop frequencies of both bands (not shown here for lack of space). The worst-case gain for the Ku-band occurred at 12.75 GHz and horizontal polarization with a deviation of 4 dB below the simulated gain of 14.41 dBi. The best case Ku-band gain occurred at 10.7 GHz and vertical polarization with a deviation of only 1 dB below the simulated gain of 12.85 dBi. This is coherent with the fact that dissipative circuit losses and reflective connector losses increase with frequency. The worst case in Ku-band cross polariza-

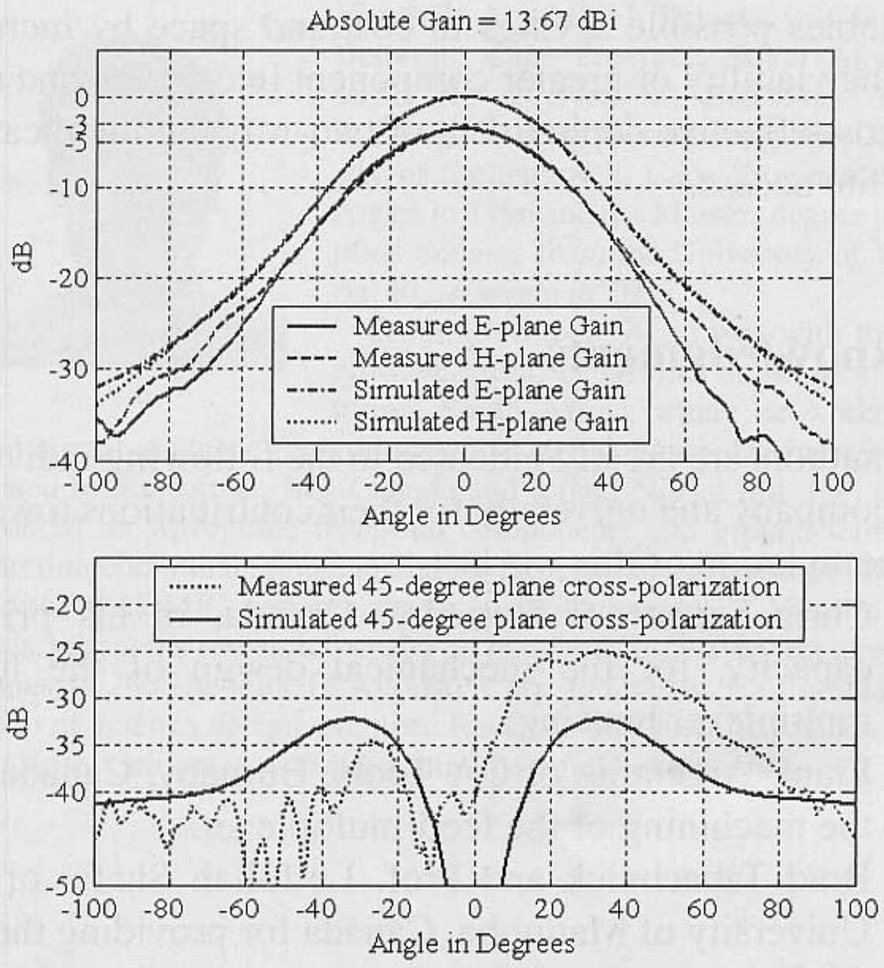

Fig. 9. Ku-band's verical polarization: Measured and simulated radiation patterns at 11.725 GHz; (a) co-polarization and gain, (b) cross polarization.

tion was found 22 dB below the measured boresight gain at 12.75 GHz horizontal polarization. Best case was 25 dB below the measured Ku-band boresight gain for a number of the patterns as is the case in the figures shown.

C) Ka-band patterns

Figs. 10 and 11 show the Ka-band radiation patterns at the mid-band frequency. The best-case Ka-band gain shows 1 to 2 dB of deviation from the simulated boresight gains of approximately 16 dBi on a number of the patterns. The worst case occurred at 29.75 dB for both polarizations with a deviation of 3 dB from the simulated boresight gain of approximately 17dB (Figs. 10 and 11). The best case Ka-band cross polarization was at 30 GHz for vertical polarization at 20 dB below the measured boresight gain and the worst case occurred at 29.5 GHz horizontal polarization at 15 dB below the measured boresight gain. This value was measured at the lobe present for both polarizations in all the Ka-band cross polarization measurements between 0 degrees and 20 degrees. This indicates a possible asymmetry in the manufactured prototype, since the polarization is switched by rotating the WR28 rotation plate and not the entire feed component.

The measured co-polarized patterns in Figs. 10a and 11a show a 2-3dB difference compared to simulations. Moreover, greater deviation in H- and E-plane beam symmetry and ripple with increasing frequency is observed (not shown here). We attribute this deviation as follows: First, the end of the dielectric rod is located slightly inside the horn aperture, thus causing moding that increases with frequency, as also experienced in [4]. Secondly, the rod should be designed at the highest frequency of operation since the rod radiation response breaks down above this frequency [8]. The extra boundary condition of the surrounding waveguide (horn) modifies the response such that it worsens with increasing frequency. Therefore, the next design cycle should compensate by designing for an even higher initial frequency.

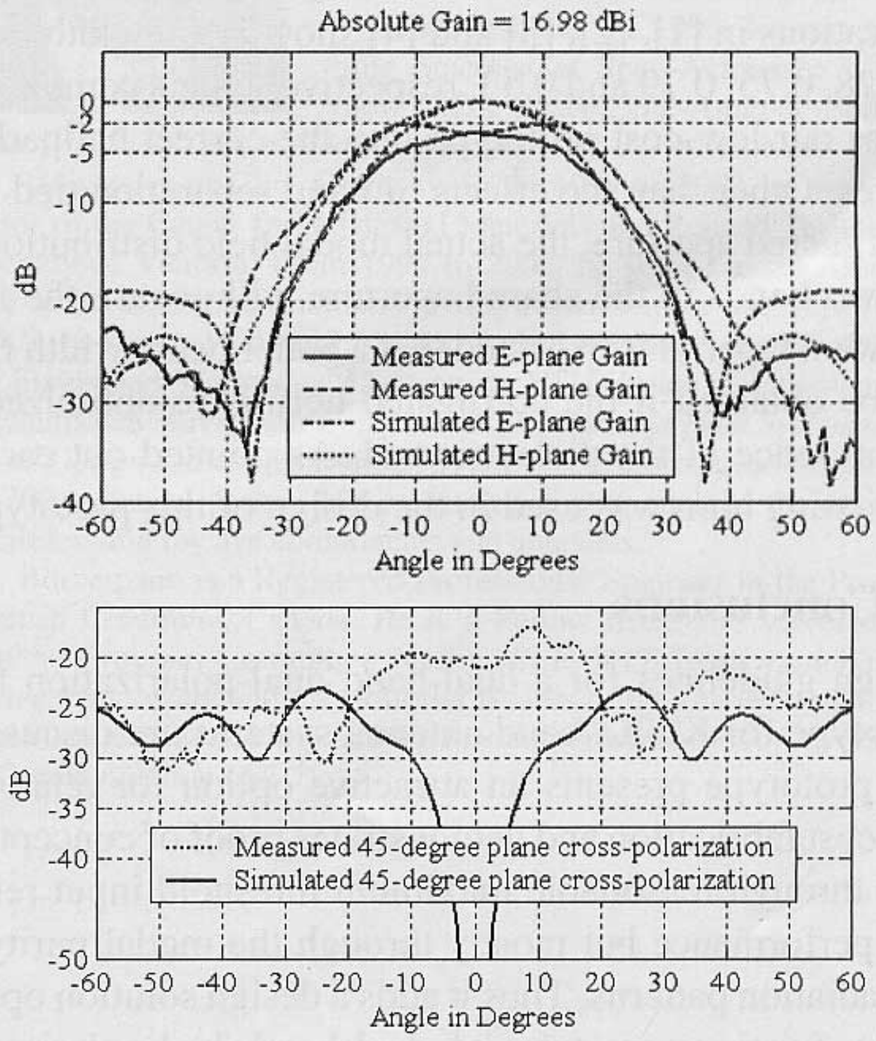

Fig. 10. Ka-band's horizontal polarization: Measured and simulated radiation patterns at 29.75 GHz; (a) co-polarization and gain, (b) cross polarization.

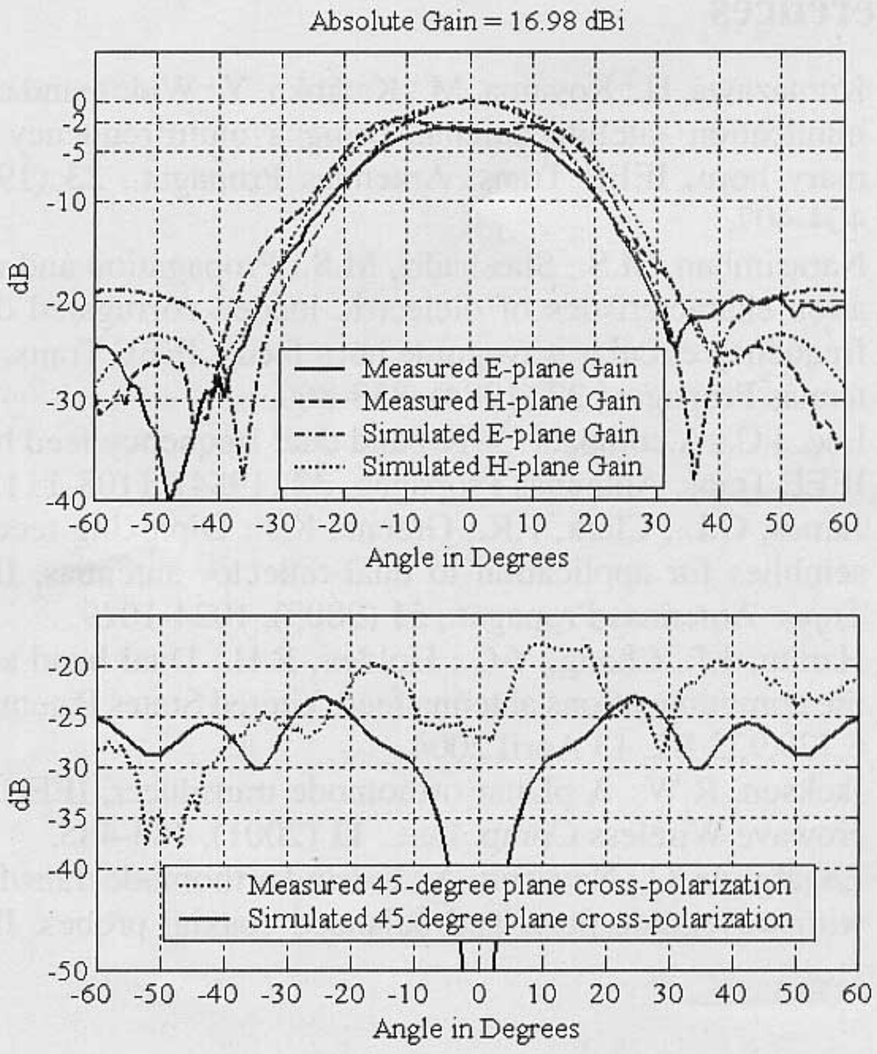

Fig. 11. Ka-band's vertical polarization: Measured and simulated radiation patterns at 29.75 GHz; (a) co-polarization and gain, (b) cross polarization.

Note that the Ka- and Ku-band patterns have different beam widths. This is expected as both signals utilize the

same aperture. For an f/d design of 0.6, the narrower Ka-band will have degraded aperture efficiency with a possibility of a better side lobe response. Obviously, the frequency separation of the bands plays a role. Based on 10 dB beam widths, the prototype presented here achieves a ratio of $24^o/37^o$=0.65. Other designs with similar band separations in [1], [2], [3] and [4] show beam width ratios of 0.78, 0.75, 0.79 and 0.53, respectively. This comparison places our low-cost prototype into the correct ballpark of figures. Other than the effects of band separation tied to a fixed shared aperture, the actual modal field distribution of the two bands in the shared aperture will govern the feed radiation taper. It is expected that a better beam width ratio can be obtained if the corrugated horn is re-optimized in the presence of the dielectric rod. As pointed out earlier, an existing horn was used in the design of this prototype.

V. Conclusions

Design guidelines for a dual-band dual-polarization feed prototype for Ku/Ka-band antenna systems are discussed. The prototype presents an attractive option for relatively low-cost fabrication and demonstrates proof of concept not only through reasonable maximum threshold input return loss performance but mostly through the modal purity of the radiation patterns. Thus it adds a design solution option to the existing repertoire of dual-band dual-polarization feed components. It enables possible savings in cost and space by increasing the viability of greater component integration and aids the cost-effective deployment of two-way communication satellite access.

Acknowledgments

The authors are greatly indebted to the following individuals, company and university for their contributions towards the completion of this work:

- Chris Senger of Burnaby, Canada, in his private capacity, for the mechanical design of the feed-multiplexer housing;
- Frank Argentine of CA Tools, Burnaby, Canada for the machining of the feed-multiplexer.
- Brad Tabachnick and Prof. Lotfollah Shafai of the University of Manitoba, Canada for providing the radiation pattern and gain measurements.
- Bruce Veidt of the National Research Council of Canada, Dominion Radio Astrophysical Observatory and Peter Haubrich of the Okanagan Valley Research and Innovation Centre, Canada for their assistance with preliminary radiation pattern measurements on the prototype.
- Norsat Intl. Inc., Burnaby, Canada for the provision of materials and the Ku-band corrugated horn.

References

[1] Kumazawa, H.; Koyama, M.; Kataoka, Y.: Wide-band communication satellite antenna using a multifrequency primary horn, IEEE Trans. Antennas Propagat., **23** (1975), 404-407.

[2] Narasimhan, M.S.; Sheshadri, M.S.: Propagation and radiation characteristics of dielectric loaded corrugated dual-frequency circular waveguide horn feeds, IEEE Trans. Antennas Propagat., **27** (1984), 858-860.

[3] Lee, J.C.: A compact Q-/K-band dual frequency feed horn, IEEE Trans. Antennas Propagat., **32** (1984), 1108-1111.

[4] James, G.L.; Clark, P.R.; Greene, K.J.: Diplexing feed assemblies for application to dual-reflector antennas, IEEE Trans. Antennas Propagat., **51** (2003), 1024-1029.

[5] Hanlin, J.J., Chang, Y-C.; Holden, R.H.: Dual band satellite comminucations antenna feed, United States Patent, US 6,729,933 B2, 13 April 2004.

[6] Jackson, R.W.: A planar orthomode transducer, IEEE Microwave Wireless Comp. Lett., **11** (2001), 483-485.

[7] Engargiola, G.; Navarrini A.: K-band orthomode transducer with waveguide ports and balanced coaxial probes, IEEE Trans. Microwave Theory Tech., **53** (2005), 1792-1801.

[8] Johnson, R.C.; Jasik, H.: Antenna Engineering Handbook, New York: McGraw-Hill, 2^{nd} ed., 1984.

[9] Kajfez, D.; Guillon, P.: Dielectric Resonators, Boston: Artech House, 1986.

[10] Thiart, H.A.: A Dual-Band and Dual-Polarization Feed-Multiplexer for Ku/Ka-Band Operation, MASc Thesis, Department of Electrical and Computer Engineering, University of Victoria, BC, Canada, 2005.

[11] Clarricoats, P.J.B; Taylor, B.C.: Evanescent and propagating modes of dielectric-loaded circular waveguide, Proc. IEE, **111** (1964), 1951-1956.

[12] Shih, Y.-C.; Ton, T.-N.; Bui, L.Q.: Waveguide-to-microstrip transitions for millimeter-wave applications, IEEE MTT-S Int. Microwave Symp. Dig., New York, May 1988, 473-475.

[13] Leong, Y.-C.; Weinreb, Y.-C.: Full-band waveguide-to-microstrip probe transitions, IEEE MTT-S Int. Microwave Symp. Dig., Anaheim, CA, June 1999, 1435-1438.

[14] Pozar, D.M.: Microwave Engineering, New York: John Wiley and Sons, 1998.

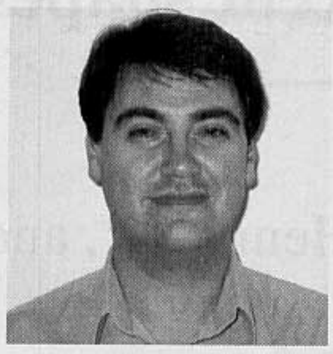

Hendrik A. (Albie) Thiart was born in Bellville, Cape Province, South Africa in 1971. He received his Bachelors degree in Electrical Engineering from the University of Stellenbosch, Cape Province, South Africa in 1996 and the Masters degree in Applied Science from the University of Victoria, BC, Canada in 2005.

From 1996 to 1999 he was with the microwave group of Grintek Avitronics, Centurion, South Africa, where he worked on hybrid circuit switches for military radar applications. During 1999 he relocated to Vancouver, BC, Canada and joined Norsat Intl. Inc. where he worked on waveguide front-end components and ground terminals for satellite communications, including project management. In 2003 he joined the CADMIC research group at the University of Victoria, BC, Canada, where his research focused on passive microwave structures and antennas. In 2005 he joined CALAMP Corp. in Oxnard, California in the position of antenna design engineer. Recently he joined Adventenna Inc. in San Jose, California working again in the field of antennas.

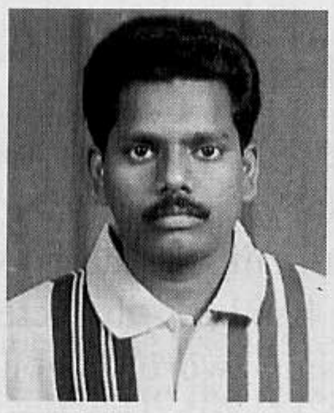

K. Rambabu completed his Ph.D. at the University of Victoria, Canada in 2004. At present he is working as a research staff at the Institute for Infocomm Research, Singapore. He has authored or coauthored over 40 papers published in refereed journals and conferences. He holds a patent for beam shaping of a cellular base station antenna. His research interests include design and development of miniaturized passive microwave components and antennas for various applications.

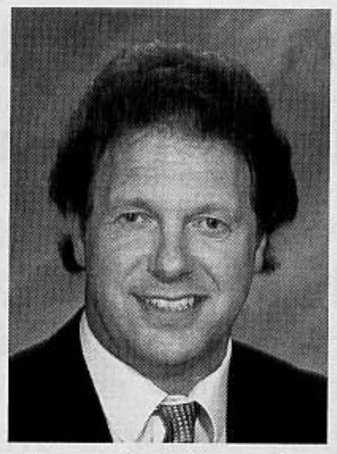

Jens Bornemann received the Dipl.-Ing. and Dr.-Ing. degrees in 1980 and 1984, respectively.

Since 1988, he has been with the Department of Electrical and Computer Engineering, University of Victoria, Victoria, B.C., Canada. From 1992 to 1995, he was a Fellow of the British Columbia Advanced Systems Institute. In 1996, he was a Visiting Scientist at Spar Aerospace Limited (now MDA Space), Ste-Anne-de-Bellevue, Québec, Canada, and a Visiting Professor at the Microwave Department, University of Ulm, Germany. From 1997 to 2002, he was a co-director of the Center for Advanced Materials and Related Technology, University of Victoria. From 1999 to 2002, he served as an Associate Editor of the *IEEE Transactions on Microwave Theory and Techniques*. In 2003, he was a Visiting Professor at the Laboratory for Electromagnetic Fields and Microwave Electronics, ETH Zurich, Switzerland. He has coauthored *Waveguide Components for Antenna Feed Systems. Theory and Design* (Artech House, 1993) and has authored/coauthored more than 200 technical papers. His research activities include the design of RF/wireless/microwave components and antennas.

Dr. Bornemann is a Registered Professional Engineer in the Province of British Columbia, Canada. He is a Fellow IEEE and serves on the Technical Program Committee of the *IEEE MTT-S International Microwave Symposium* and the Editorial Boards of the *International Journal of Numerical Modelling* and the *International Journal of Electronics and Communication (AEÜ)*.